Ultralow-loss Waveguide Crossings for the Integration of Microfluidics and Optical Waveguide Sensors

Zheng Wang*[a,b], Hai Yan[b], Zongxing Wang[c], Yi Zou [b], Chun-Ju Yang [b], Swapnajit Chakravarty*[c], Harish Subbaraman[c], Naimei Tang [c], Xiaochuan Xu[c], D.L. Fan[a,d], Alan X. Wang[e] and Ray T. Chen*[a,b,c]

[a]Materials Science and Engineering Program, Texas Materials Institute, The University of Texas at Austin, Austin, TX USA 78712;

[b]Dept. of Electrical and Computer Engineering, The University of Texas at Austin, 10100 Burnet Rd., MER 160, Austin, TX USA 78758;

[c]Omega Optics, Inc., 8500 Shoal Creek Blvd., Bldg. 4, Suite 200, Austin, TX USA 78757;

[d]Dept. of Mechanical Engineering, University of Texas at Austin, Austin, TX USA 78712;

[e]School of Electrical Engineering and Computer Science, Oregon State University, Corvallis, OR USA 97331

ABSTRACT

Integrating photonic waveguide sensors with microfluidics is promising in achieving high-sensitivity and cost-effective biological and chemical sensing applications. One challenge in the integration is that an air gap would exist between the microfluidic channel and the photonic waveguide when the micro-channel and the waveguide intersect. The air gap creates a path for the fluid to leak out of the micro-channel. Potential solutions, such as oxide deposition followed by surface planarization, would introduce additional fabrication steps and thus are ineffective in cost. Here we propose a reliable and efficient approach for achieving closed microfluidic channels on a waveguide sensing chip. The core of the employed technique is to add waveguide crossings, i.e., perpendicularly intersecting waveguides, to block the etched trenches and prevent the fluid from leaking through the air gap. The waveguide crossings offer a smooth interface for microfluidic channel bonding while bring negligible additional propagation loss (0.024 dB/crossing based on simulation). They are also efficient in fabrication, which are patterned and fabricated in the same step with waveguides. We experimentally integrated microfluidic channels with photonic crystal (PC) microcavity sensor chips on silicon-on-insulator substrate and demonstrated leak-free sensing measurement with waveguide crossings. The microfluidic channel was made from polydimethylsiloxane (PDMS) and pressure bonded to the silicon chip. The tested flow rates can be varied from 0.2 μL/min to 200 μL/min. Strong resonances from the PC cavity were observed from the transmission spectra. The spectra also show that the waveguide crossings did not induce any significant additional loss or alter the resonances.

Keywords: Biological sensing and sensors, Detection, Photonic crystals, Subwavelength structures, Microfludics

1. INTRODUCTION

Microfluidic channel systems have shown unique advantages in performing analytical functions such as controlled transportation, immobilization, and manipulation of biological molecules and become an essential part of modern nanotechnology research [1]. On the other hand, chip integrated photonic sensors, utilizing microring resonators [2], 2D photonic crystal [3], wire waveguides [4], etc., have enabled label free and high sensitivity sensing with ultra-compact size and low cost. By integrating microfluidics with photonic sensors, one may gain more benefits like reduced sample consumption, shorter analysis time, higher sensitivity, portability, etc. More importantly, micro-fluid channel system is a necessary technique for achieving integrated biosensors [5]. Our previous work has already demonstrated high sensitivity photonic crystal chemical sensors [6], enhanced sensitivity photonic crystal biosensors [7] and plasmonic-active surface enhanced Raman spectroscopy systems[8]. While sensing characteristics can in general be demonstrated by dispensing analytes of interest via pipettes, when binding kinetics needs to be measured for instance in the case of biosensors for drug discovery applications, a continuous flow of analyte must be reliably achieved.

*wangzheng@utexas.edu; swapnajit.chakravarty@omegaoptics.com; raychen@uts.cc.utexas.edu

Microfluidics, BioMEMS, and Medical Microsystems XIII, edited by Bonnie L. Gray, Holger Becker
Proc. of SPIE Vol. 9320, 932012 · © 2015 SPIE · CCC code: 1605-7422/15/$18
doi: 10.1117/12.2078384

A conventional optical waveguide is characterized by cross-section such as J-J' shown in Fig. 1(a). Optical waveguides are in general laid out such that the fluids flow orthogonal to the direction of optical wave propagation. Thus, as noted in the right image in Fig. 1(b), an air gap would exist between the PDMS mold (PDMS being the material of choice for microfluidic channels) and the bottom silicon dioxide cladding in a silicon-on-insulator (SOI) substrate. One typical solution to close the avenue for fluid leakage in silicon chip integrated waveguide sensor is introducing additional fabrication steps including but not limited to oxide deposition followed by planarization and selective oxide removal prior to microfluidic channel bonding [9]. In the case of photonic crystal sensors, such post processing would necessitate removal of the oxide from the etched photonic crystal patterns which would result in additional etching of the bottom oxide cladding unless the process is very strictly controlled. A poor tolerance on the oxide removal processing would lead to uncertain resonance wavelengths in photonic crystal biosensors. Recently, photonic crystal devices have been fabricated using photolithography [10]. However, additional fabrication steps associated with oxide deposition, planarization and removal need additional photo masks which translate to higher manufacturing cost.

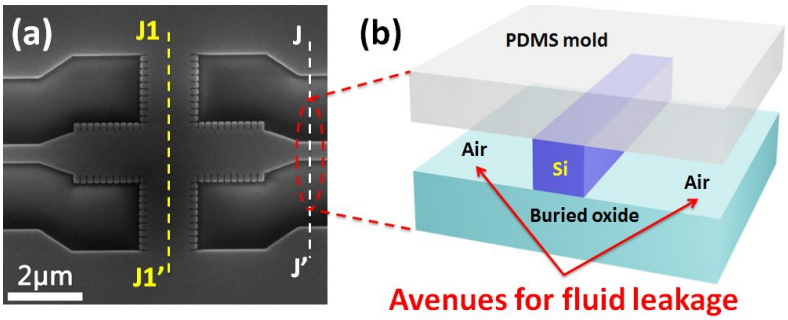

Fig. 1.(a)SEM image of a typical waveguide crossing and conventional waveguides are characterized by cross-sections J-J'. (b) Cross-sectional view of the PDMS microfluidic channel when integrated with optical waveguides in silicon in a SOI substrate.

In this paper, we demonstrate an approach using ultralow-loss silicon waveguide crossings to build a closed micro-fluid channel with leak-free integrated fluidics operation. The microfluidic channel is designed so that channel walls go over the section J1-J1' in Fig. 1(a) which effectively closes the gaps that would otherwise exist in the channel along J-J', in the absence of waveguide crossings. This novel approach is extremely fabrication friendly, since the primary ridge waveguides, photonic crystals and crossing waveguides are fabricated in the same step with a single photomask, and also offers a smooth interface excluding additional planarization process for microfluidic channel bonding.

2. DESIGN AND SIMULATION

A cascaded MMIs structure, whose top-view schematic is shown in Fig. 2(a), is utilized to build ultra-low loss waveguide crossings on a SOI substrate (3 μm thick buried oxide layer and 250 nm thick top silicon layer) since it enables guiding of low-loss Bloch waves by periodic self-focusing sections offered by MMIs [11]. Commercial available software FIMMWAVE (developed by Photon Design Ltd.) is used for simulation and a side view schematic of the simulated structure is shown Fig. 2(b). Here the W_{si} is chosen to be 0.6 μm to build a single-mode waveguide and W_{mmi} is chosen as 1.2 μm to support only three quasi-TE modes (zeroth, first and second). As the symmetry of this structure, the odd first-order mode is not been excited. Hence the self-focusing condition can be perfectly fulfilled by tuning L_{in} and L_s to eliminate the phase error between zeroth and second mode. Linear tapers (L_t= 1μm) are added to avoid sharp transition and at the same time to reduce the portion of the power in second-order mode in the MMI region which could improve the power transition [12]. Effective medium theory is utilized to calculate the cladding index (n_c) around the crossing region which provides a minimal modal phase noise, thus lowering the propagation loss at the crossing region. Theoretically, one can drive the phase error of the m^{th} mode $\Delta\varphi_m$ at the N-folding imaging length as

$$\Delta\varphi_m \approx \frac{P}{4}\frac{\lambda_0^2\left(\mathrm{m}+1\right)^4\pi}{2Nn_f^2W_{e0}^2}\left[\frac{1}{8}-\frac{\lambda_0 n_f^2}{6\pi W_{e0}\left(n_f^2-n_c^2\right)^2}\right] \quad (1)$$

where P is the number of self-imaging periods, λ_0 is the optical wavelength, We_0 is the is the effective width of the MMI for the zeroth mode, n_f is the effective refractive index of the fundamental mode of infinite slab waveguides with the same thickness as the MMI and n_c is the lateral cladding index[11]. Specifically speaking, the increasing of n_c will reduce the TM component of quasi-TE mode both in single-mode ridge waveguide and MMI region. Thus the power transition between the two waveguides will be improved at the input and output. Fig. 2(c) shows a scan of the cladding index (n_c) which indicates that n_c~2.5 is sufficient to provide the lowest loss result. The propagation field profile of 20 waveguide crossings with the optimized parameters: n_c~2.5, L_{in}= 2.16 μm, L_s= 1.58 μm is shown in Fig. 2(d) and the propagation loss is 0.0241dB per crossing.

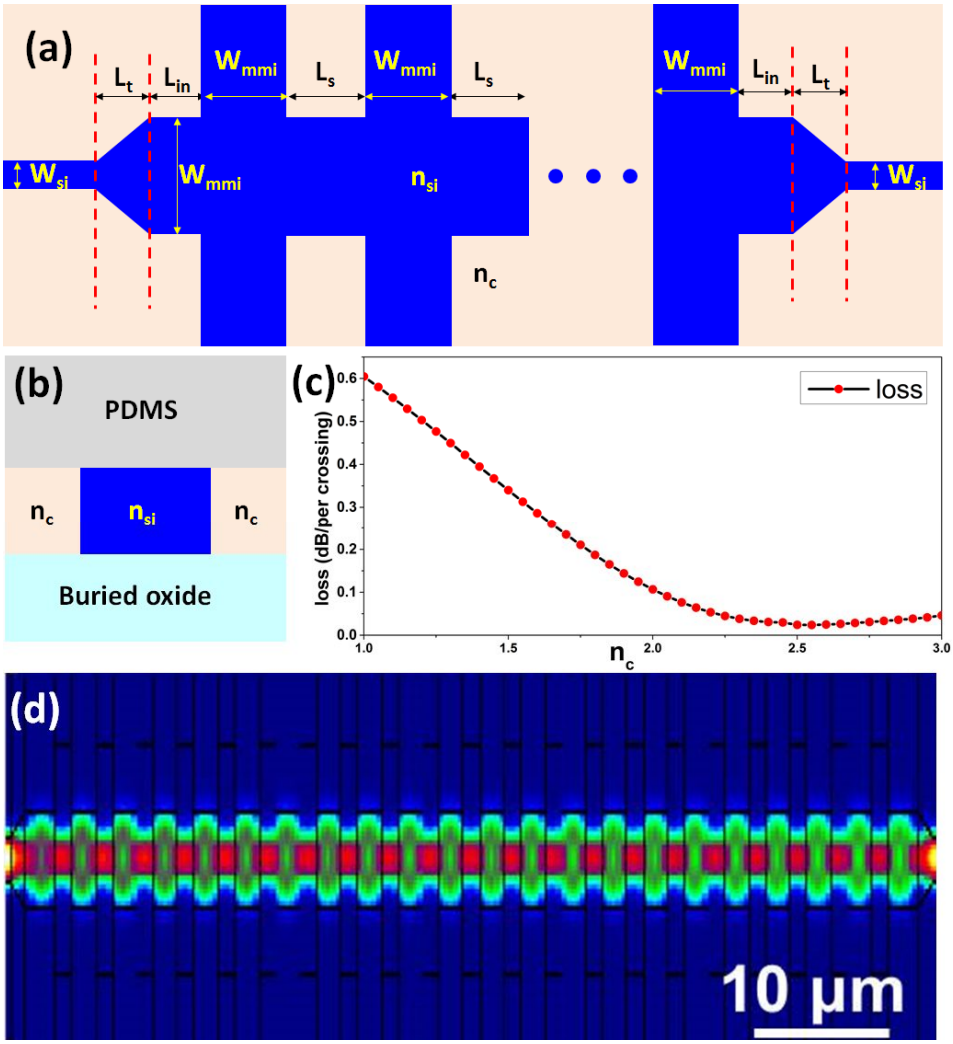

Fig. 2. (a) Top-view schematic of cascaded MMI-based waveguide crossings. (b) Side view schematic of simulated structure. (c) Simulated propagation loss versus lateral cladding index for the structure in (a). (d) FIMMWAVE simulation result of 20 waveguide crossings with optimized parameters.

3. FABRICATION AND INTEGRATION

In order to demonstrate the effectiveness of the waveguide crossings in preventing the leaking problem as well as its compatibility with photonic sensors, we integrate waveguide crossings with our matured L55 photonic crystal microcavity sensor [13]. The 3D schematic of the integrated device, which the PDMS based microfluidic channel has already been bonded onto the sensor chip, is shown in the left image of Fig. 3 and an exploded view 3D schematic illustrating components of the integrated device is shown in the right one. The photonic crystal microcavity sensor sits at the center integrated with the primary ridge waveguide. Waveguide crossings are located on both sides of the photonic crystal sensor where the PDMS wall of the microfluidic channel is placed. Subwavelength gratings [14] are used to couple light in and out between silicon waveguide and optical fibers.

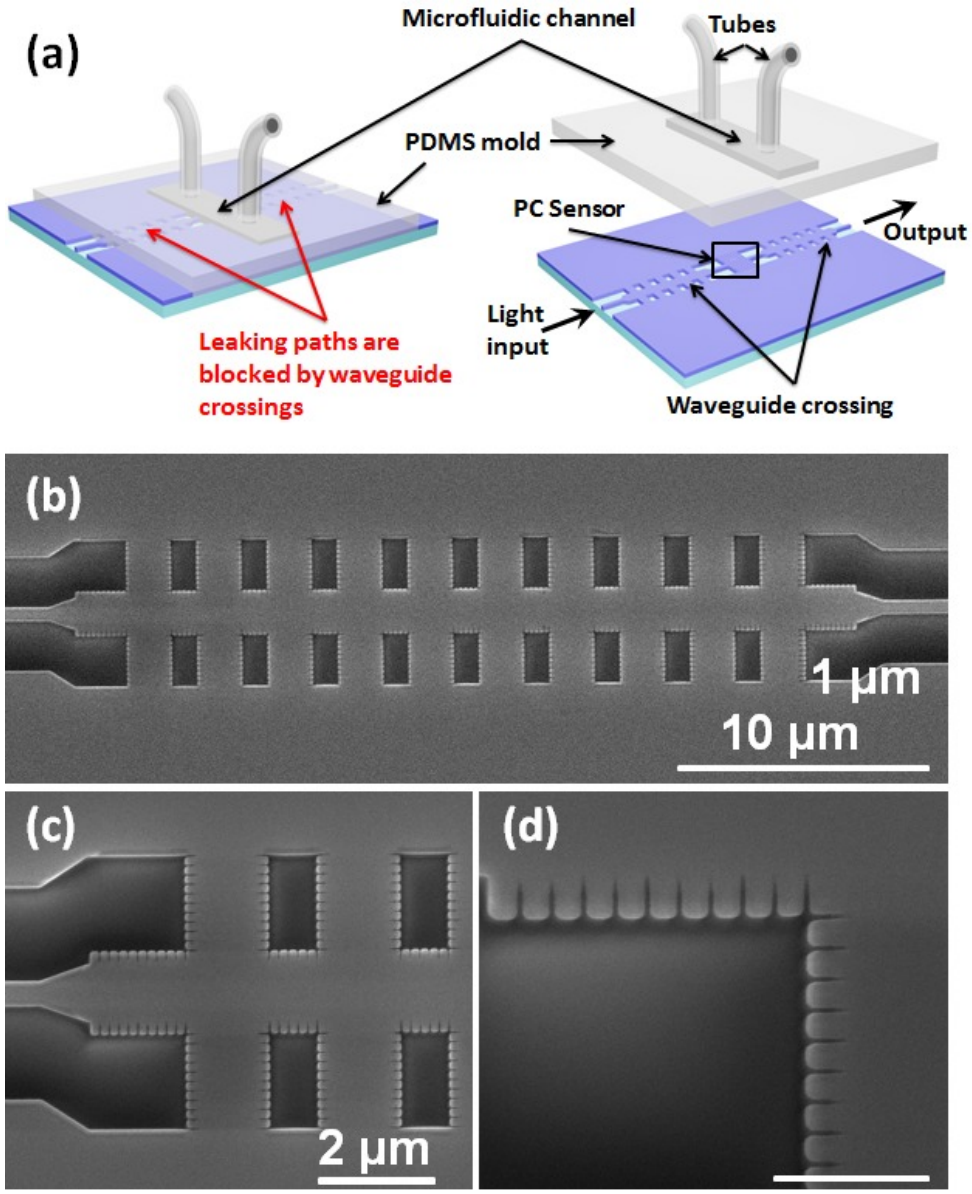

Fig. 3. (a) 3D schematic of the integrated device. (b)-(d) SEM images of fabricated waveguides crossings.

All structures, including primary ridge waveguides, photonic crystal waveguides and microcavity, waveguide crossings and subwavelength grating couplers, are patterned in one electron-beam lithography step. The pattern was then transferred to silicon layer through reactive-ion-etch (RIE). SEM images of fabricated waveguide crossings are shown in Fig. 4(a)-(c). Those tooth-like subwavelength nanostructures are used to make an artificial material with desired lateral cladding index n_c ~2.5 [15].

The microfluidic channel was fabricated using PDMS following standard soft lithography technique [16]. Briefly, a 50 μm thick SU-8 photoresist was spin-coated on a silicon wafer. The microfluidic channel pattern was transferred to the photoresist layer using photolithography through a Mylar mask. After development, a SU-8 layer is used to mold PDMS. PDMS was poured on to a polished Si wafer and polymerized in an oven at 70 °C for 2 hours. Later, two holes were punctured at each end of the microfluidic channel as inlet and outlet ports for tubes connection. The microfluidic channel fabricated is 1 mm wide and 15 mm long. The PDMS mold embedded with microfluidic channels aligning with the sensor chip is shown in Fig. 4(a).

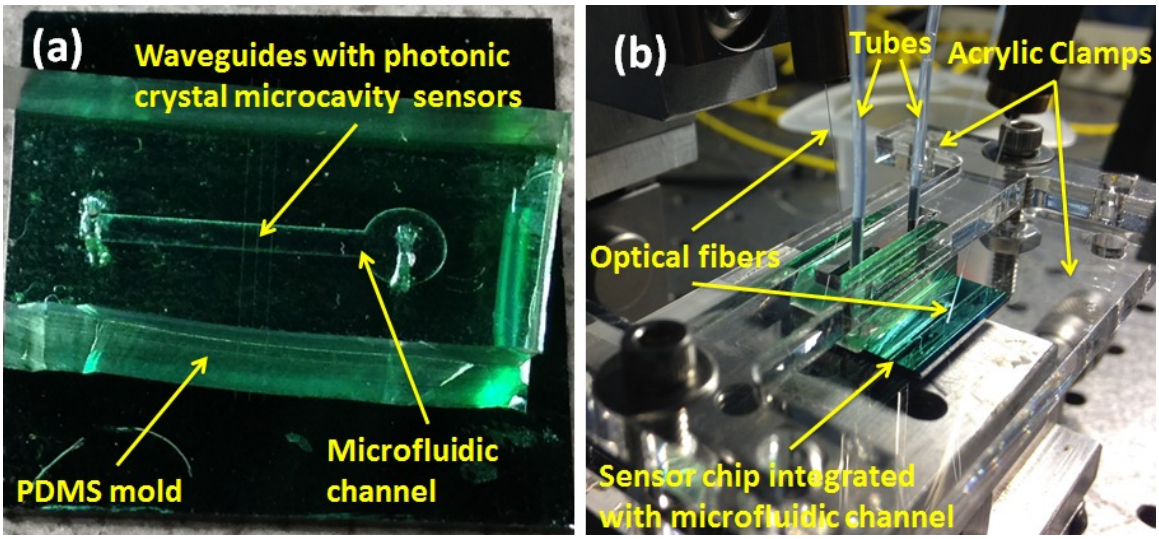

Fig. 4.(a) Picture of a device with PDMS microfluidic channel. (b) Picture of the measurement setup.

Here we use pressure-bonding technique inspired by Quan et al. [17]. For biosensing, PDMS is accepted universally as a bio-compatible microfluidic channel material. However, PDMS cannot serve as a channel material for organic solvents. Furthermore, new materials are being designed as an alternative to PDMS to achieve better wetting characteristics of channel walls. The use of pressure bonding allows any suitable choice of microfluidic channel material other than PDMS, without the need for new process development. The PDMS mold with microfluidic channel was aligned to the silicon chip and then clamped together by two pieces of laser cut acrylic glass. In our experiment it was found that the increasing of pressure, which was applied by screwing more tightly, would lead a decreasing of the minimum number of waveguide crossings to build a fully closed environment. Thus by applying higher pressure results in a drop of propagation loss with fewer waveguide crossings. Theoretically, a large enough deformation of PDMS induced by clamps with ultra-high pressure might close the 250 nm deep air trench even without waveguide crossings; however the high stress status carried by chip and clamps makes the whole device extremely vulnerable to mechanical cracking and is thus unstable. To balance the higher risk of mechanical failure versus the lower propagation loss caused by application of stronger clamping pressure, 10 waveguide crossings were added on both sides of the PC microcavity sensor (20 crossing waveguides in total). The sensor chip integrated with microfluidic channel and clamps were placed on an optical stage for fiber to grating coupler alignment and transmission spectrum measurement. The setup is shown in Fig. 4(b). Solution was introduced into the channel by a syringe pump (Harvard Apparatus). Light from a LED source (DenseLight Semiconductors) was coupled into the sensor waveguide through a grating coupler to stimulate quasi-TE mode. On the output port, light was coupled out into an optical spectrum analyzer to obtain the transmission spectrum.

4. EXPERIMENTAL VALIDATION

Considering that PDMS has an absorption effect in our interesting wavelength regime [18], devices first were tested in DI-water without and with PDMS mold to show the effect caused by PDMS absorption. Transmission spectra were shown in Fig. 5(a) and strong resonance peaks are observed. The propagation loss caused by the PDMS mold could be neglected as the planar favored energy distribution of quasi-TE mode. The same device was next tested in glycerol to validate operation as a chemical sensor. Experiment results are shown in Fig. 5(b). The shift of the transmission spectrum is 7.1 nm corresponding to the refractive index change[19].

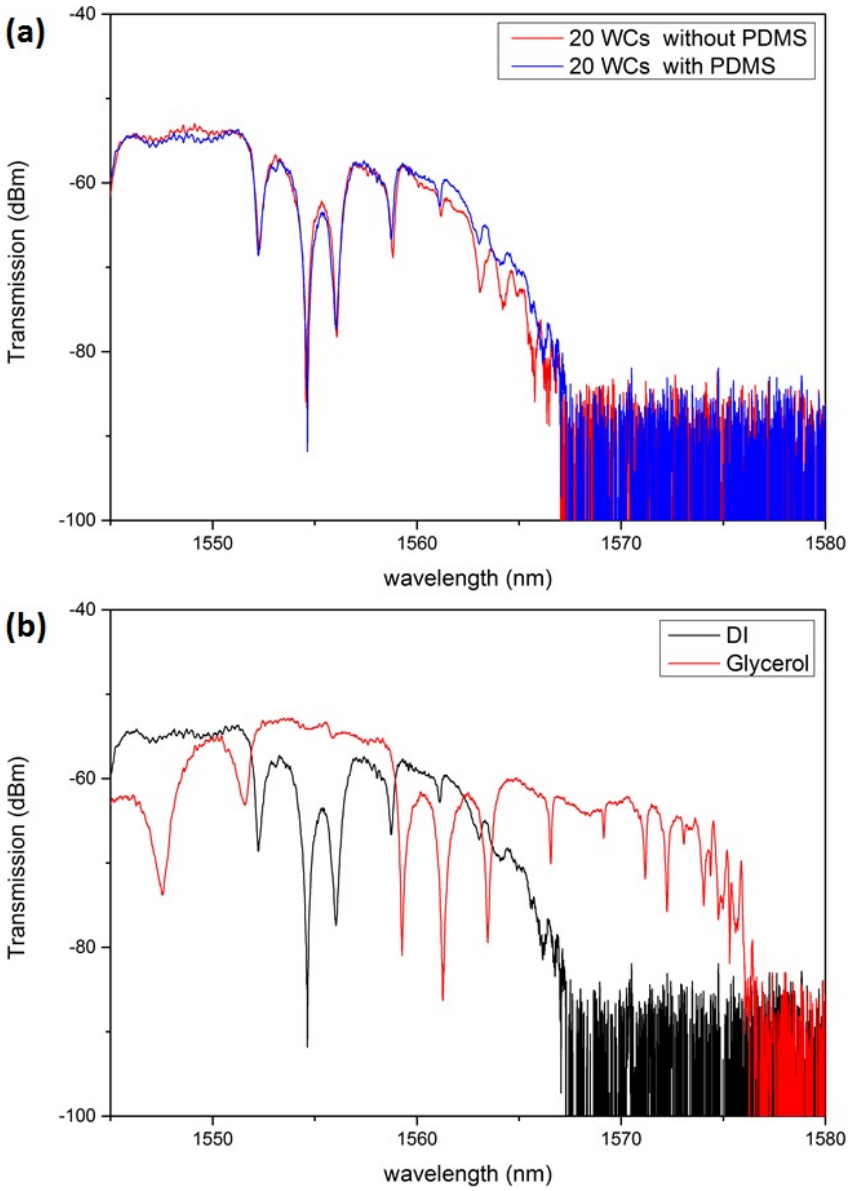

Fig. 5.(a) Spectra of L55 photonic crystal microcavity sensor with 10 waveguide crossings on both sides with and without PDMS microfluidic channel. (b) Spectra of L55 photonic crystal microcavity sensor tested in DI water and glycerol.

5. CONCLUSION

In conclusion, we integrated waveguide crossings into the chip-based waveguide sensor that enables leak-free operation of microfluidic channels. This process is compatible with existing SOI micro-fabrication technique and requires no additional fabrication step. Also this scheme is suitable for various sensing application that uses optical waveguides and need microfluidic channel to deliver the media to be tested.

ACKNOWLEDGEMENTS

The authors acknowledge the National Institutes of Health for sponsoring this research under SBIR grant 5R42ES024023-03 and 9R42ES024023-02.

REFERENCES

[1] Hong, J. W., and Quake, S. R., "Integrated nanoliter systems," Nat. Biotechnol., 21(10), 1179-1183 (2003).
[2] Washburn, A. L., Gunn, L. C., and Bailey, R. C., "Label-Free Quantitation of a Cancer Biomarker in Complex Media Using Silicon Photonic Microring Resonators," Anal. Chem., 81(22), 9499-9506 (2009).
[3] Pal, S., Guillermain, E., Sriram, R., Miller, B. L., and Fauchet, P. M., "Silicon photonic crystal nanocavity-coupled waveguides for error-corrected optical biosensing," Biosens. Bioelectron., 26(10), 4024-4031 (2011).
[4] Densmore, A., Vachon, M., Xu, D. X., Janz, S., Ma, R., Li, Y. H., Lopinski, G., Delage, A., Lapointe, J., Luebbert, C. C., Liu, Q. Y., Cheben, P., and Schmid, J. H., "Silicon photonic wire biosensor array for multiplexed real-time and label-free molecular detection," Opt. Lett., 34(23), 3598-3600 (2009).
[5] Erickson, D., and Li, D. Q., "Integrated microfluidic devices," Ana. Chim. Acta., 507(1), 11-26 (2004).
[6] Lai, W. C., Chakravarty, S., Zou, Y., and Chen, R. T., "Multiplexed detection of xylene and trichloroethylene in water by photonic crystal absorption spectroscopy," Opt. Lett., 38(19), 3799-3802 (2013).
[7] Lai, W. C., Chakravarty, S., Zou, Y., Guo, Y. B., and Chen, R. T., "Slow light enhanced sensitivity of resonance modes in photonic crystal biosensors," Appl. Phys. Lett., 102(4), (2013).
[8] Xu, X. B., Hasan, D. H., Wang, L., Chakravarty, S., Chen, R. T., Fan, D. L., and Wang, A. X., "Guided-mode-resonance-coupled plasmonic-active SiO2 nanotubes for surface enhanced Raman spectroscopy," Appl. Phys. Lett., 100(19), (2012).
[9] Ruano, J. M., Benoit, V., Aitchison, J. S., and Cooper, J. M., "Flame hydrolysis deposition of glass on silicon for the integration of optical and microfluidic devices," Anal. Chem., 72(5), 1093-1097 (2000).
[10] Yang, C.-j., Tang, N., Yan, H., Chakravarty, S., Li, D., and Chen, R., "193nm Lithography Fabricated High Sensitivity Photonic Crystal Microcavity Biosensors for Plasma Protein Detection in Patients with Pancreatic Cancer," OSA Technical Digest (online).
[11] Zhang, Y., Hosseini, A., Xu, X. C., Kwong, D., and Chen, R. T., "Ultralow-loss silicon waveguide crossing using Bloch modes in index-engineered cascaded multimode-interference couplers," Opt. Lett., 38(18), 3608-3611 (2013).
[12] Chen, C. H., and Chiu, C. H., "Taper-Integrated Multimode-Interference Based Waveguide Crossing Design," IEEE J. Quantum. Elect., 46(11), 1656-1661 (2010).
[13] Zou, Y., Chakravarty, S., Kwong, D. N., Lai, W. C., Xu, X. C., Lin, X. H., Hosseini, A., and Chen, R. T., "Cavity-Waveguide Coupling Engineered High Sensitivity Silicon Photonic Crystal Microcavity Biosensors With High Yield," IEEE J. Sel. Top. Quantum Electron., 20(4), (2014).
[14] Xu, X. C., Subbaraman, H., Covey, J., Kwong, D., Hosseini, A., and Chen, R. T., "Complementary metal-oxide-semiconductor compatible high efficiency subwavelength grating couplers for silicon integrated photonics," Appl. Phys. Lett., 101(3), 031109 (2012).

[15] Ortega-Monux, A., Zavargo-Peche, L., Maese-Novo, A., Molina-Fernandez, I., Halir, R., Wangumert-Perez, J. G., Cheben, P., and Schmid, J. H., "High-Performance Multimode Interference Coupler in Silicon Waveguides With Subwavelength Structures," IEEE. Photonic. Tech. L., 23(19), 1406-1408 (2011).
[16] Unger, M. A., Chou, H. P., Thorsen, T., Scherer, A., and Quake, S. R., "Monolithic microfabricated valves and pumps by multilayer soft lithography," Science, 288(5463), 113-116 (2000).
[17] Yang, D. Q., Kita, S., Liang, F., Wang, C., Tian, H. P., Ji, Y. F., Loncar, M., and Quan, Q. M., "High sensitivity and high Q-factor nanoslotted parallel quadrabeam photonic crystal cavity for real-time and label-free sensing," Appl. Phys. Lett., 105(6), (2014).
[18] Cai, D. K., Neyer, A., Kuckuk, R., and Heise, H. M., "Optical absorption in transparent PDMS materials applied for multimode waveguides fabrication," Opt. Mater., 30(7), 1157-1161 (2008).
[19] Chakravarty, S., Hosseini, A., Xu, X. C., Zhu, L., Zou, Y., and Chen, R. T., "Analysis of ultra-high sensitivity configuration in chip-integrated photonic crystal microcavity bio-sensors," Appl. Phys. Lett., 104(19), (2014).